



Type of the Paper (Article)

Application of infrared and nuclear magnetic resonance spectra in studying the bacterial efficacy of some oxazepane derivatives derived from hydrazones

Abdul Wahed Abdul Sattar Talluh^{1*}, Mohammed Jwher Saleh² and Jamil Nadhem Saleh³

¹ Tikrit University, College of Basic Education, Shirqat, Tikrit University, Iraq

² Salah al-Din Education Directorate, Iran

³ Salah al-Din Education Directorate, Iraq

Corresponding Author: ikbaliqbalhabdulkareem@gmail.com

Received date: 03/09/2024; Accepted date: 29/09/2024; Published date: 30/09/2024

Abstract: This research included the utilisation of infrared and nuclear magnetic resonance spectra in studying and preparing new derivatives of the oxazepan ring by a series of reactions, where the triazole ring was prepared from the reaction of the carboxylic acid with carbothiohydrazide, and from the resulting reaction (triazole) with aqueous hydrazine. The latter was reacted with benzaldehyde compensators to prepare hydrazones, which is the basic intermediate for the preparation of the oxazepan ring. The hydrazones were reacted with succinic anhydride, and the validity of the structures was proven using infrared and nuclear magnetic resonance spectra of proton and carbon. Its biological activity has also been tested for two species of Gram-positive bacteria, *Staphylococcus epidermidis* and Gram-negative *Klebsiella pneumoniae*.

Keywords: Infrared spectra; triazole; hydrazide; hydrazone; oxazepane; biological activity.

1. Introduction

The Heterocyclic compound consists of nitrogen, oxygen, and sulphate atoms in addition to carbon atoms [1]. Heterocyclic compounds are widely distributed in nature, as they enter into the composition of many organic compounds necessary for the basic formation of life, and they are also found in different forms in sugars and their derivatives [2]. Triazole, a heterocyclic organic compound containing nitrogen currently receiving attention due to its biological, industrial, and medical importance, is 2,14-triazole, as triazole is a five-membered ring containing three nitrogen atoms and two nitrogen atoms. Carbon atoms can contain two types of bonds, as the nucleus of 1,3,4-triazole has antimicrobial effects and treats hypoglycemia and hypertension [3]. Where the number (1) gives the nitrogen atom to which the hydrogen atom is attached to distinguish it. Triazole compounds, in which the nitrogen atoms are not linked to each other because they are separated by two carbon atoms, are named as follows: 1,3,4-triazole. It also gives the nitrogen atom to which it is attached. The number of hydrogen atoms (1), and the two carbon atoms (5, 2) with substituents [4].

Hydrazides and their derivatives are important intermediates used in the preparation of many heterocyclic organic compounds, as they are intermediates in the preparation of many



compounds, such as Schiff bases, due to their biological activity [5]. Hydrazones are organic compounds resulting from the condensation reaction between the hydrazine compound and various aldehydes or ketones, which occurs through an unstable intermediate state to a product known as hydrazone, which consists of 2 nitrogen atoms; the first is hydrogen, and the second is the hydrazone. The nitrogen atom. The second is linked to the carbon atom by bonding the hydrazone carrying the functional group (-HC=N-NH-C=O) [6]. Hydrazones and their derivatives have recently received great attention after the discovery of the biological effects of this compound. They are extensively applied in medical and pharmaceutical fields and have also been used as antifungals [7] and antibacterials [8]. Oxazepane contains seven atoms consisting of 5 carbon atoms, one nitrogen atom, and one oxygen atom (90), of which 1,3- Oxazepane -7,4-dione can be manufactured by adding anhydrides such as phthalic acid or maleic acid and others. A double bond of Schiff base or isomethene (C=N) of hydrazine[9]. Oxazepane compounds also contain three isomers numbered according to the two nitrogen atoms in the ring, where the nitrogen atom is in position (2, 3, or 4) and the oxygen atom is in position (1) [10].

Oxazepane compounds have wide biological importance and have received wide attention in the medical field as they have shown antibacterial [11], anticonvulsant [12], and antioxidant [13].

2. Materials and Methods

2.1. Used Chemicals: All used chemicals supplied by Aldrich, BDH Thomas, Fluka, and Merck were used.

2.2. Instruments used: The melting point was ascertained using a Shimadzu-8400S FT-IR spectrometer, a 400-4000 cm^{-1} sulfur bromide disk, a 9300 thermometer, and 400 MHz Bruker ^1H - and ^{13}C -NMR spectra. The catalyst surface was verified by SEM examination. Fluka silica gel plates 0.02cm in thickness were used for thin-layer chromatography (TLC).

2.3. Preparation of Triazole (MH1)

Equal moles (0.003 mol) of carboxylic acid were mixed with hydrazine carbothiohydrazide in a heat-resistant vessel without solvent, stirring for 10 minutes until the colour changed. The resulting compound was collected and recrystallised from ethanol, giving a yellow colour with a product yield of 83% M.p 149-151 [14].

2.4. Preparation of Hydrazide (MH2)

Equal moles (0.002 mol) of triazole MH1 were mixed with 98% aqueous hydrazine in a vessel; 20 ml of CS_2 was added, stirring for 10 minutes. The resulting material was collected and recrystallised from ethanol, giving an orange colour with a yield of 79% M.p 176-178 [15].

2.5. Preparation of Hydrazones (MH3-MH7)

The resulting hydrazide MH2 was mixed with the benzaldehyde substitutes in a vessel in equal molar ratios (0.003 mol) without solvent, stirring for 8 minutes [16]. The resulting material was then collected and recrystallised from ethanol, as in Table 1.



Table (1): Some physical characteristics of the synthesised compound (MH3-MH7).

Compound	R	Molecular formulas	m.p. °C	Yield %	Colour
MH3	4-Br	C ₁₈ H ₁₄ BrN ₇ S ₂	197-199	68	Yellow
MH4	4-NO ₂	C ₁₈ H ₁₄ N ₈ S ₂ O ₂	188-190	64	Brown
MH5	4-Cl	C ₁₈ H ₁₄ ClN ₇ S ₂	203-205	71	Whit
MH6	4-OH	C ₁₈ H ₁₅ N ₇ S ₂ O	200-202	63	Dark Yellow
MH7	4-H	C ₁₈ H ₁₅ N ₇ S ₂	191-193	60	Blue

2.6. Preparation of Oxazepane (MH8-MH12)

In a heat-resistant vessel, equal moles (0.006 mol) of the prepared hydrazones (MH3-MH7) were mixed with succinic anhydride without solvent, stirring for 15 min [17]. The material was then collected and recrystallised from ethanol, as in Table 2.

Table (2): Some physical characteristics of the synthesised compound (MH8-MH12).

Compound	R	Molecular formulas	m.p. °C	Yield %	Colour
MH8	4-Br	C ₂₂ H ₁₈ BrN ₇ O ₃ S ₂	221-223	64	Light Yellow
MH9	4-NO ₂	C ₂₂ H ₁₈ N ₈ O ₅ S ₂	234-236	62	Dark Brown
MH10	4-Cl	C ₂₂ H ₁₈ ClN ₇ O ₃ S ₂	237-239	68	Yellow
MH11	4-OH	C ₂₂ H ₁₉ N ₇ O ₄ S ₂	243-245	73	Yellow
MH12	4-H	C ₂₂ H ₁₉ N ₇ O ₃ S ₂	226-228	71	whit

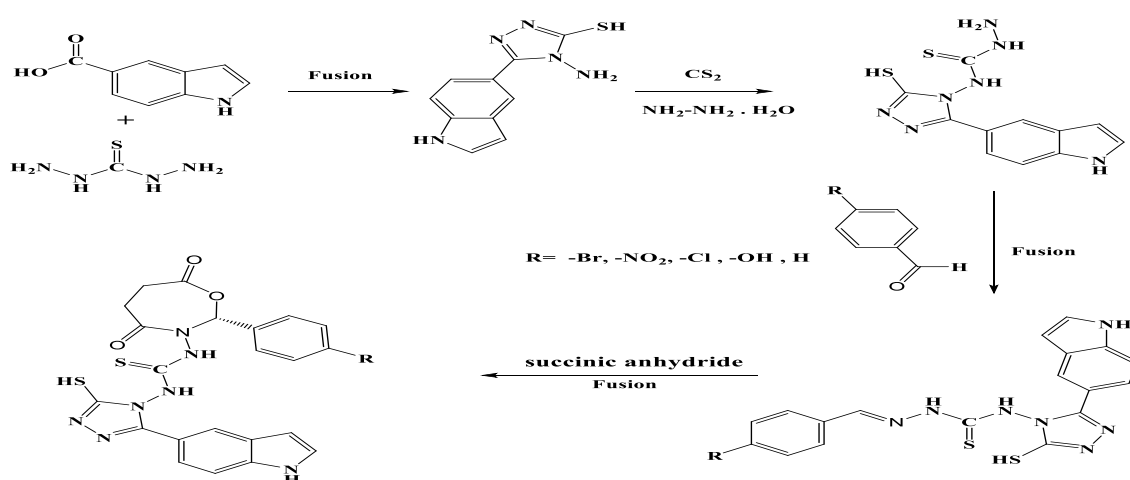
2.7. Study of biological activity

Two colonies of pure bacterial isolates of both Gram-positive *Staphylococcus epidermidis* and Gram-negative *Klebsiella pneumoniae* were transferred from the solid culture medium to test tubes containing (5 ml) distilled water using heat-sterilised holders [18,19]. The tubes were incubated at 37°C for 16-20 hrs and then diluted using a physiological solution until the turbidity reached standard turbidity levels to obtain a cell count of approximately (1.5×10⁸) cells/ml. Chemical solutions of some of the synthesised compounds were prepared using dimethyl sulfoxide (DMSO) solvent at three concentrations (0.1, 0.01, 0.001) mg.mL⁻¹ of each substance (for each solid derivative). Agar-Miller-Hinton (MHA) medium was introduced into a test tube containing diluted bacterial growth [20,21]; the swab was pressed against the inner walls of the tube to remove the extra inoculums, followed by inoculation with a sterile swab. In order for the inoculum to be evenly distributed [22-24].



3. Results

The synthesised compounds are shown in Scheme 1.



Scheme (1): Path of the ready compounds (MH1-MH12).

After the subsection, please use the bullet points if you require any further breakdown, i.e.

3.1. Characterisation of Triazole (MH1).

The FT-IR spectrum of MH1 showed that the absorption bands of rubber (NH_2) were present between 3431 and 3335 cm^{-1} , and the absorption bands were present at position 3191 cm^{-1} . For rubber (NH), the band at 3039 cm^{-1} is attributed to the aromatic ($=\text{C}-\text{H}$) stretching, and the band at 1620 cm^{-1} belongs to the ($\text{C}=\text{N}$) stretching, and the $1485\text{-}1519\text{ cm}^{-1}$ band is attributed to the aromatic ($\text{C}=\text{C}$) stretching[25], as shown in Figure 1.

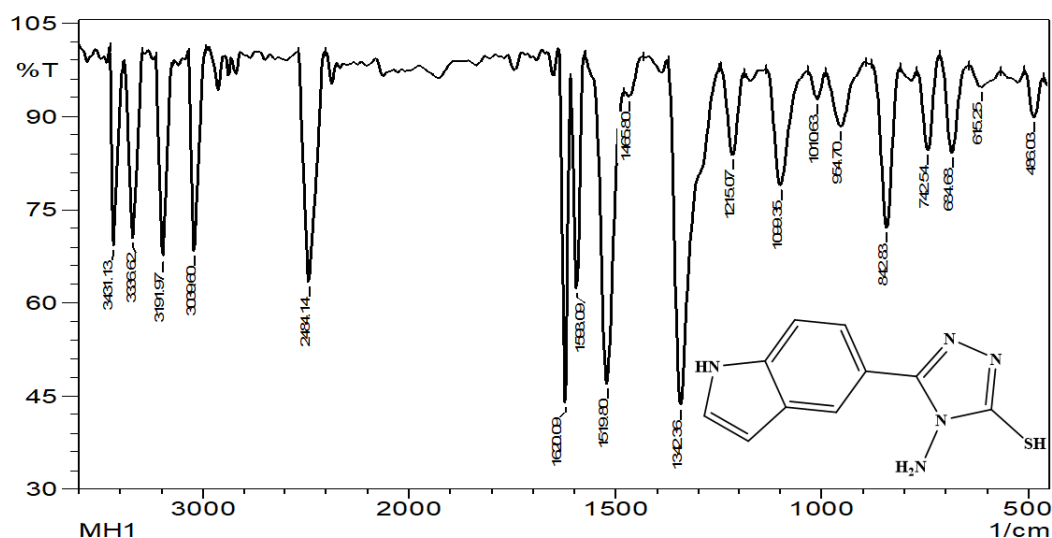
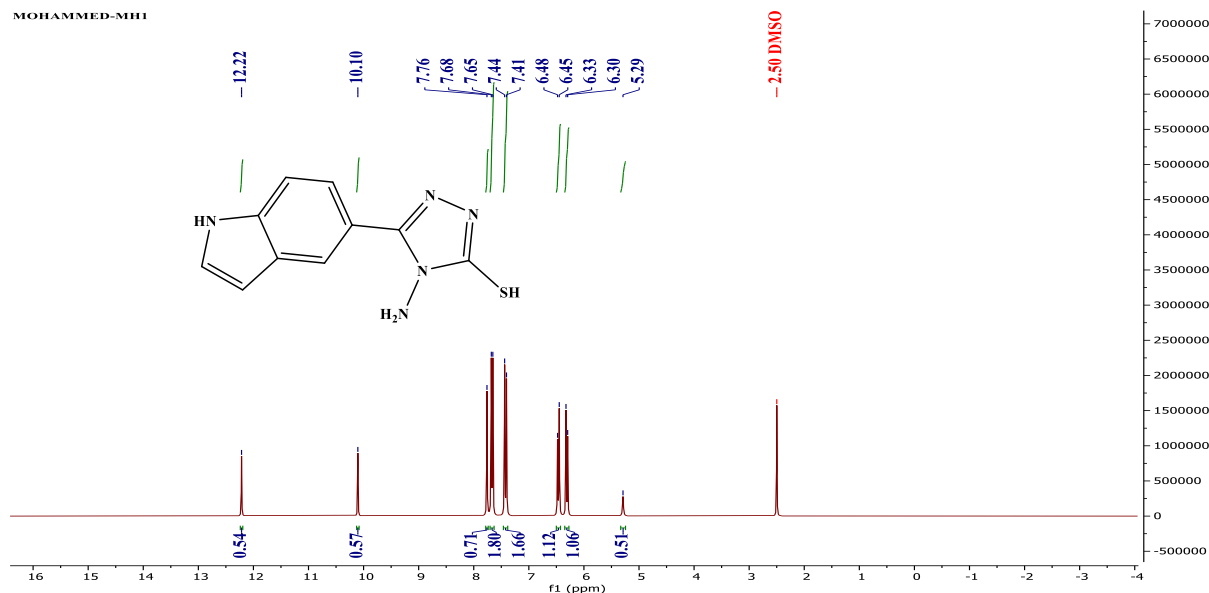


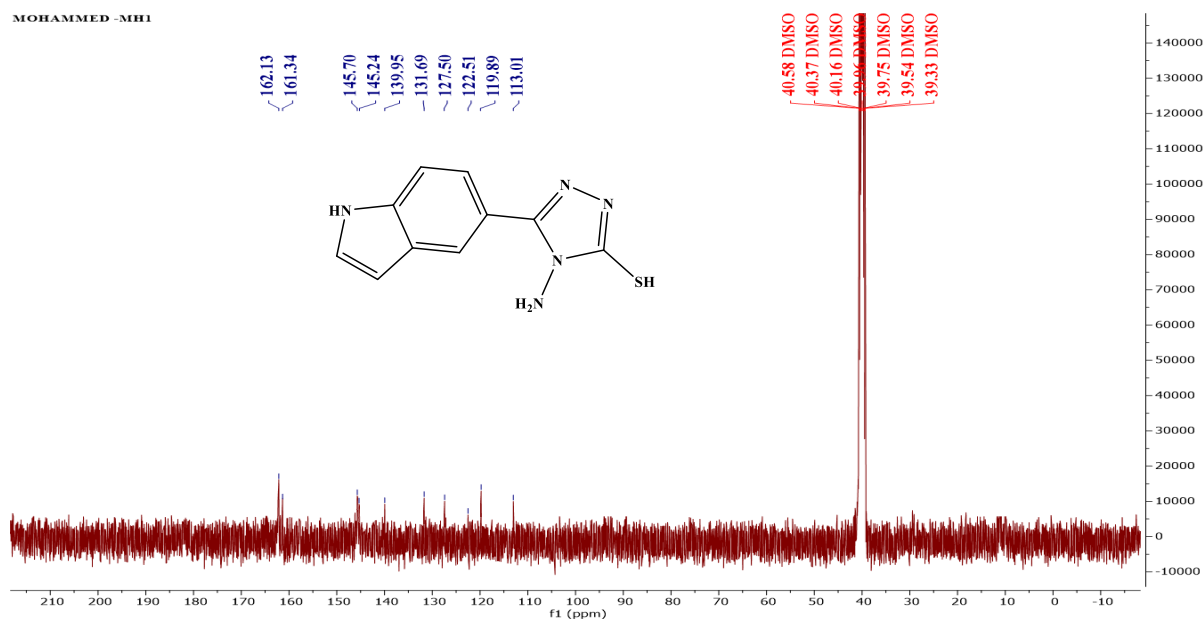
Figure (1): The compound's FT-IR spectra (MH1).



During the study of the $^1\text{H-NMR}$ spectrum of MH1, one signal was noticed at position (5.29 ppm) attributed to the proton (NH_2), and two signals shown in the range of 6.30-6.48 ppm due to the presence of a double bond ($\text{CH}=\text{CH}$), several signals in the range of 7.41-7.76 ppm attributed to the protons of the aromatic ring, signals at positions (10.10) ppm belongs to the protons (NH), and a signal at position (12.22) ppm belongs to the proton (SH), then the signal of the solvent DMSO-d^6 at position 2.50 ppm, as shown in Figure 2.



When the $^{13}\text{C-NMR}$ spectrum of MH1 was studied, two signals were observed belonging to the double bond carbon ($\text{C}=\text{C}$) at the position (113.01-119.89) ppm, signals attributed to the aromatic ring carbon in the range (122.51-145.70) ppm, and two signals attributed to the ($\text{C}=\text{N}$) triazole ring at the position (161.34-162.13) ppm. A multiple signal in the range (39.33-40.58) ppm was attributed to the carbon of the solvent DMSO-d^6 , as shown in Figure 3.





3.2. Characterisation of Hydrazone (MH2).

When studying the infrared spectrum of (MH2) compounds, it was found that a band is formed in the region $(1616) \text{ cm}^{-1}$ due to $(\text{C}=\text{N})$ stretching, and the absorption band in the region $(3344\text{--}3303) \text{ cm}^{-1}$, which resulted, is often attributed to (NH_2) stretching, and a band at the site $(3238, 3180) \text{ cm}^{-1}$ is due to (NH) , and the aromatic $(\text{C}\text{--}\text{H})$ stretching is responsible for the absorption band in the region $(3002) \text{ cm}^{-1}$. The two absorption bands at $(1093) \text{ cm}^{-1}$ are usually because of the $\text{C}=\text{S}$ stretching, and the two bands are because of the aromatic $(\text{C}=\text{C})$ stretching in the range $(1519\text{--}1461)$ [26]. As in Figure 4

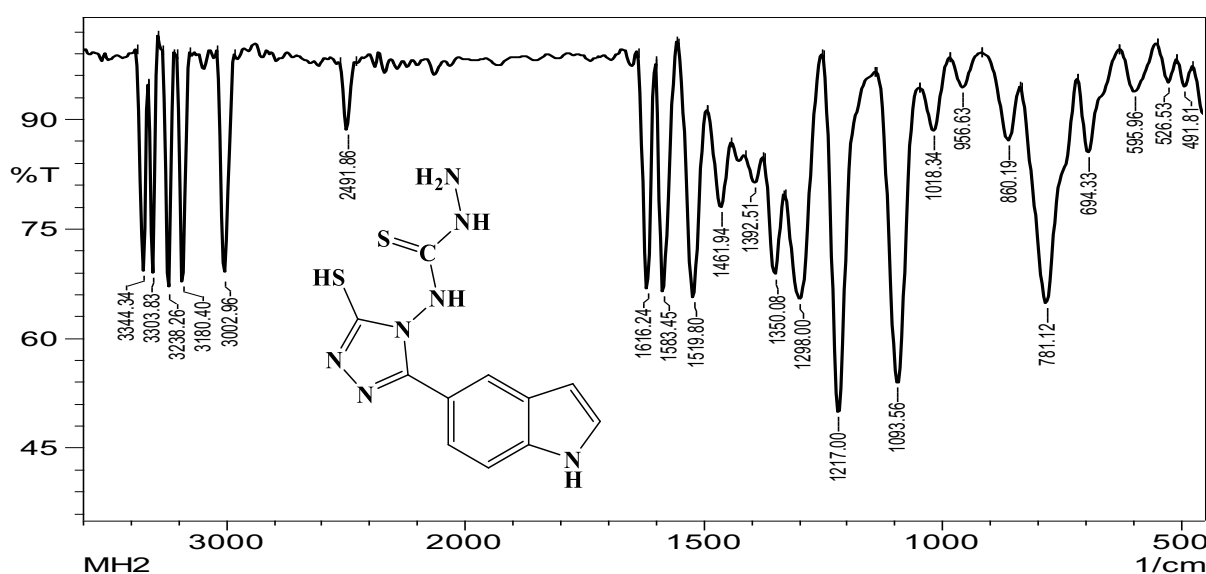


Figure (4): The compound's FT-IR spectra (MH2).

The ^1H NMR spectrum of MH2 showed one signal was at 4.26 ppm because of the presence of the NH_2 . Two signals were present between 6.53 and 6.69 ppm because of the presence of a double bond ($\text{CH}=\text{CH}$), multiple signals were present in the range of 7.34–7.63 ppm because of the protons of the aromatic ring, signals at positions (7.01) ppm attributed to the proton (NH) adjacent to the triazole ring, a signal at 8.81 ppm belongs to the proton (NH) adjacent to the amine, a signal at position (9.23) ppm attributed to the proton (NH) of the five-membered ring, a signal at 10.85 ppm attributed to the proton (SH), then the signal of the solvent DMSO- d_6 at position (2.50) ppm, see Figure 5.

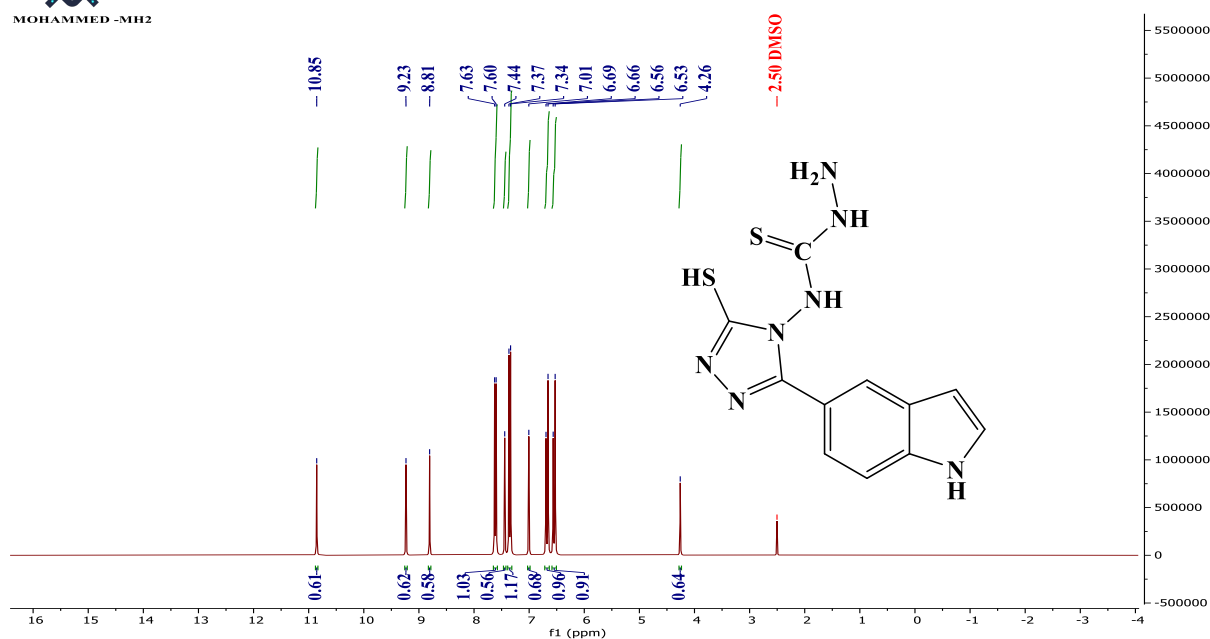


Figure (5): 1-H NMR spectra of the substance (MH2).

When studying the ^{13}C -NMR spectrum of MH2, two signals were observed belonging to the carbon of the double bond ($\text{C}=\text{C}$) at the position (112.17-113.72) ppm, two signals attributed to the carbon of the aromatic ring in the range (121.87-143.81) ppm, two signals attributed to the triazole ring ($\text{C}=\text{N}$) at the position (152.60-166.39) ppm, and a signal at the position (182.28) ppm due to the presence of $\text{C}=\text{C}$ carbon. Also, multiple signals in the range (39.54-40.59) ppm due to the presence of carbon of the solvent DMSO-d₆, as shown in Figure 6.

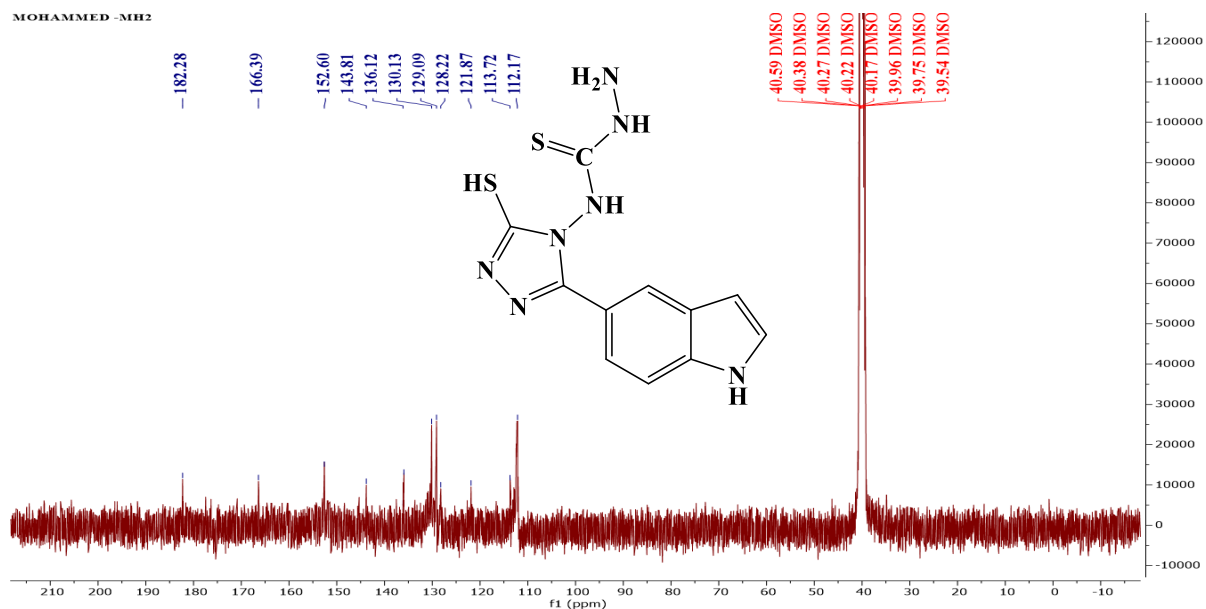


Figure (6): ^{13}C -NMR Spectra of MH2.

3.3. Characterisation of Hydrazone (MH3-MH7).

When studying the infrared spectrum of hydrazones, it was found that a band is formed between 1635 and 1626 cm^{-1} due to ($\text{C}=\text{N}$) stretching, and the resulting absorption bands between 3338 and 3232 cm^{-1} are often attributed to (NH) stretching, and the aromatic ($\text{C}-\text{H}$) stretching band is responsible for the absorption band in the range (3060 - 3027 cm^{-1}). The two



absorption bands in the range (3162-3141) cm^{-1} are usually attributed to ($=\text{C-H}$) stretching, and the two bands are attributed to aromatic (C=C) stretching in the range (1553-1458) [27]. As in Table and Figures 7 and 8.

Table (3): FT-IR absorption results for Prepared compounds (MH3-MH7)

Comp. No.	R	$\nu(\text{C-H})$ Arom.	$\nu(=\text{C-H})$ Olphen.	$\nu(\text{SH})$ $\nu(\text{C=S})$	$\nu(\text{C=N})$	$\nu(\text{C=C})$ Arom.	Others
MH3	4-Br	3060	3141	3240 2368	2368 1635	1508,145 8	$\nu(\text{C-Br})$ 659
MH4	4-NO ₂	3057	3151	3238 3293	2453 1081	1626 1600	1545,148 7 $\nu(\text{N-O})$ as sy1514. Sy1315
MH5	4-Cl	3037	3122	3251 3338	2503 1058	1635 1596	1517,146 0 $\nu(\text{C-Cl})$ 783
MH6	4-OH	3027	3147	3246 3305	2487 1075	1629 1601	1553,148 1 $\nu(\text{OH})$ 3396
MH7	4-H	3034	3162	3232 3287	2396 1069	1631 1606	1548,147 9 --

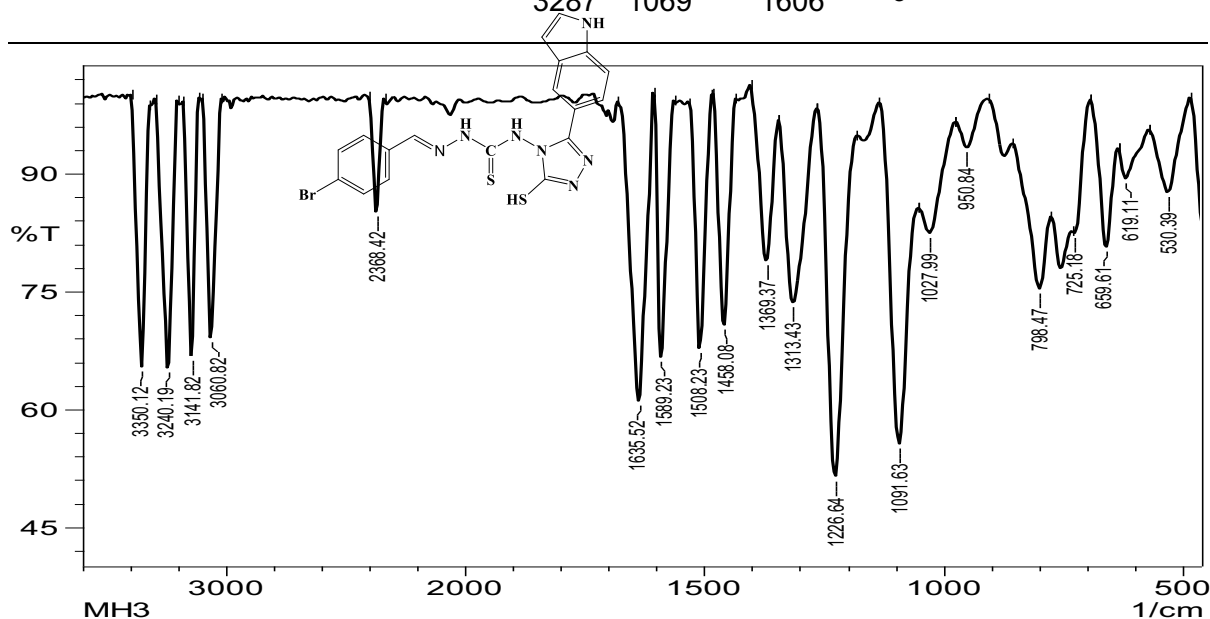


Figure (7): The compound's FT-IR spectra (MH3).

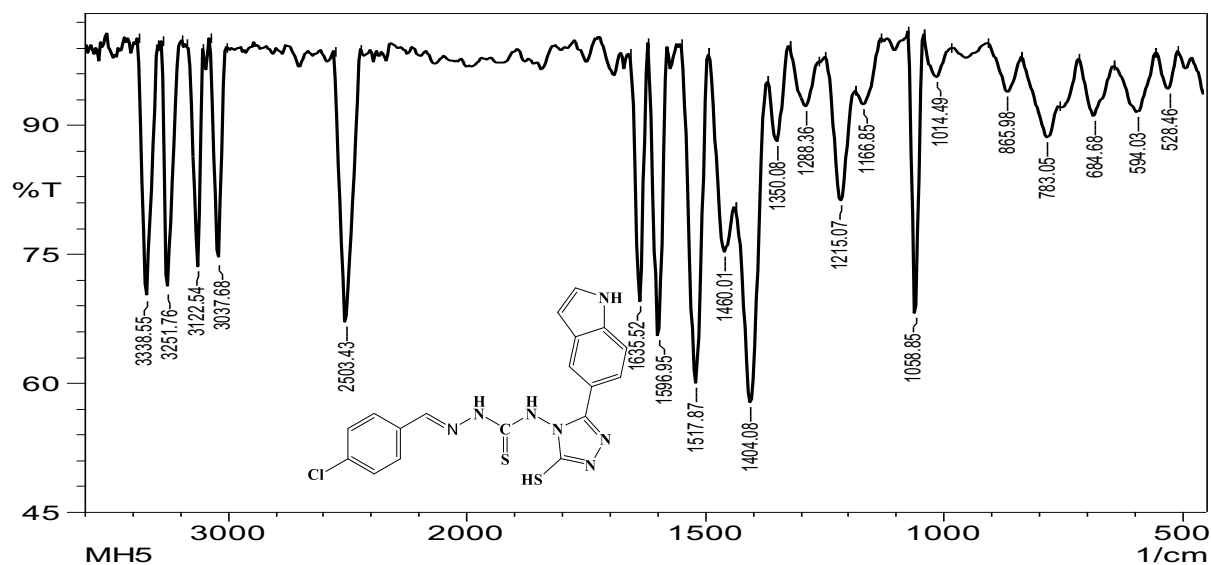


Figure (8): The compound's FT-IR spectra (MH5).

The ^1H NMR spectrum of MH2 shows two signals were noticed in the range (6.71-6.83) ppm attributed to the double bond (CH=CH), and several signals in the range (7.20-7.96) ppm because of the presence of the protons of the aromatic ring, signals at positions (7.02) ppm attributed to the proton (NH) adjacent to the triazole ring, a signal at position (8.39) ppm part of the colourant because of the presence of the proton (=CH). A signal at position (9.01) ppm because of the presence of proton (NH), a signal at position (9.98) ppm attributed to the proton (NH) of the five-membered ring, a signal at position (11.47) ppm because of the presence of proton (SH), then the signal of the solvent DMSO-d₆ at position (2.49) ppm million, see Figure 9.

MOHAMMED -MH3

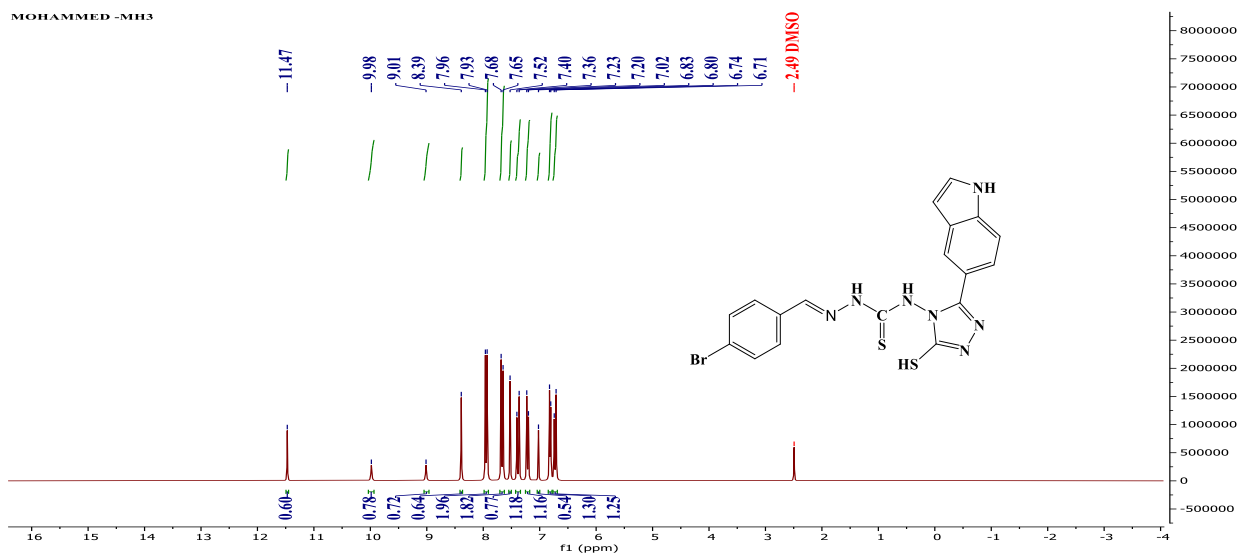


Figure (9): 1-H NMR spectra of the substance (MH5).

When studying the ^{13}C -NMR spectrum of MH3, two signals were observed belonging to the double bond carbon atom (C=C) at position (117.24-119.83) ppm, two signals attributed to the aromatic ring carbon atom in the range (121.72-136.34) ppm, a signal at position (141.34) ppm because of the formation of carbon (C=N), two signals attributed to the triazole ring (C=N) at position (154.00-161.13) ppm, and a signal at position (176.81) ppm attributed to the carbon



atom (C=S). A multiple signal was also observed in the range (39.30-40.56) ppm because of the presence of carbon atom of the solvent DMSO-d₆, as shown in Figure 10.

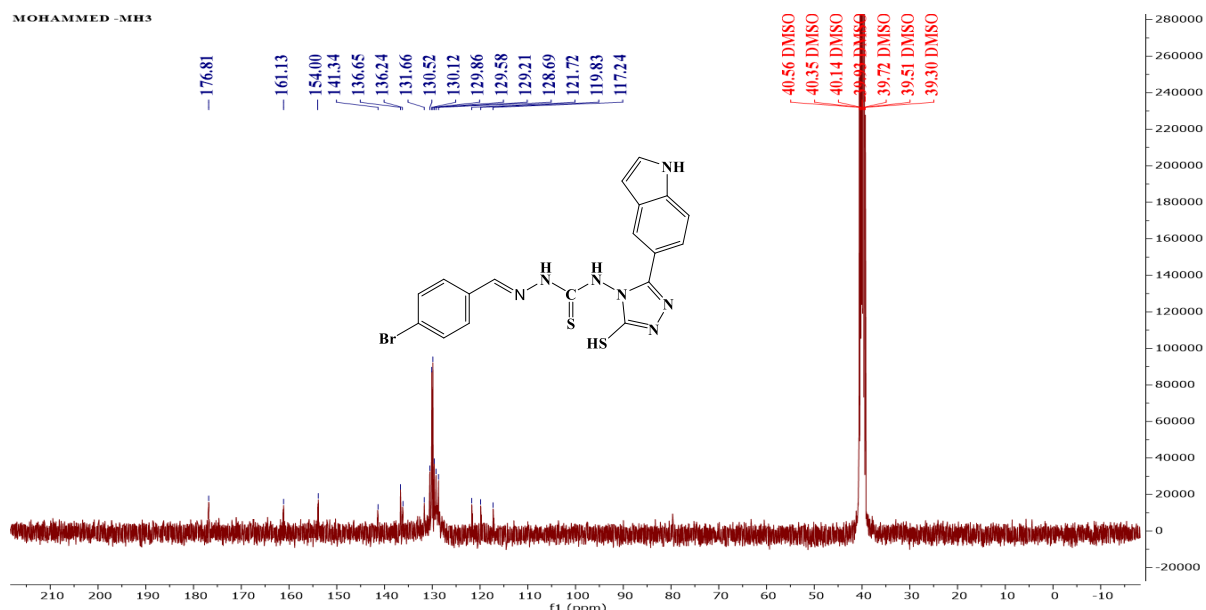


Figure (10): ¹³C-NMR Spectra of the substance (MH3).

3.4. Characterisation of Oxazepane (MH8-MH12).

In the FT-IR spectrum of Oxazepane derivatives, a band was noticed in the range (1728-1703) cm⁻¹ attributed to the ester (C=O) in the heptad ring, a band in the range (1670-1645) cm⁻¹ attributed to the imide (C=O) in the resulting ring, a band in the range (1365-1347) cm⁻¹ attributed to (C-O) in the same ring, and two bands attributed to the aliphatic (C-H) in the range (2893-2858) cm⁻¹ and (2980-2928) cm⁻¹, in addition to two bands in the range (1577-1521) cm⁻¹ and (1488-1462) cm⁻¹ attributed to the aromatic (C=C) [28]. These are shown in Table 4 and Figures 11 and 12.

Table (4): FT-IR absorption results for prepared compounds (MH8-MH12).

Comp. No.	R	$\nu(\text{C-H})$ Arom.	$\nu(\text{C-H})$ Aliph.	$\nu(\text{N-H})$	$\nu(\text{SH})$ $\nu(\text{C=S})$	$\nu(\text{C=N})$	$\nu(\text{C=C})$ Arom.	Others
MH8	4-Br	3034	2876 2943	3257 3321	1709 1654	1603 1354	1523,1476	$\nu(\text{C-Br})$ 617
MH9	4-NO ₂	3045	2893 2980	3207 3286	1728 1670	1612 1365	1577,1464	$\nu(\text{N-O})$ as sy1523. Sy1327
MH10	4-Cl	3052	2858 2928	3207 3291	1716 1649	1605 1359	1531,1483	$\nu(\text{C-Cl})$ 761
MH11	4-OH	3041	2884 2931	3246 3281	1721 1664	1606 1347	1542,1488	$\nu(\text{OH})$ 3365



MH12	4-H	3051	2885	3200	1703	1597	1521,1462	--
			2972	3298	1645	1348		

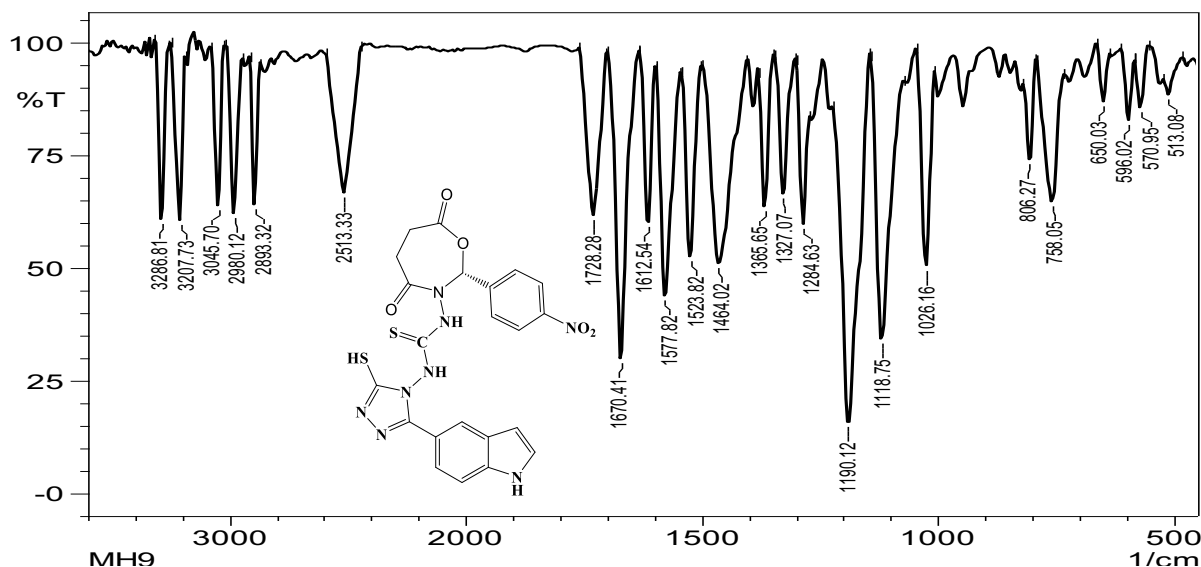


Figure (11): The compound's FT-IR spectra (MH9).

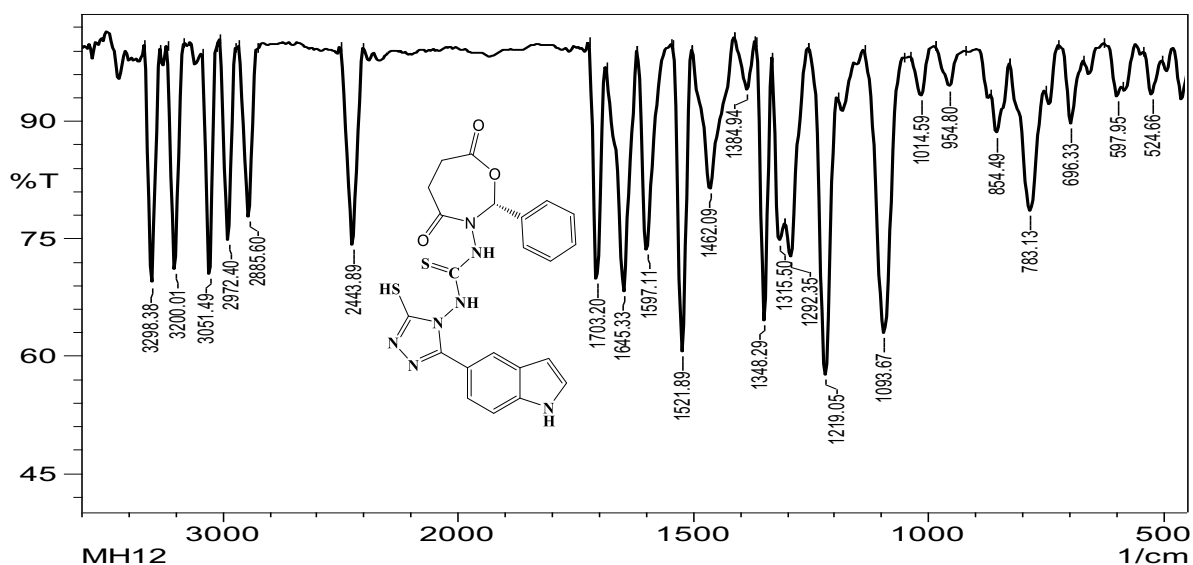


Figure (12): The compound's FT-IR spectra (MH12).

In the $^1\text{H-NMR}$ spectrum of MH10, two triple signals were observed attributed to $(\text{CH}_2\text{-CH}_2)$ in the heptad ring in the range (2.90-3.24) ppm, and a signal at (8.65) ppm because of the presence of proton (CH) in the resulting ring, in addition to two signals in the range (6.15-6.42) ppm attributed to the double bond ($\text{CH}=\text{CH}$), and several signals noticed in the range (7.19-7.95) ppm attributed to the protons of the aromatic ring, and a signal at positions (6.80) ppm because of the presence of proton (NH) adjacent to the triazole ring, and two signals at positions (9.27-9.63) ppm because of the presence of proton (NH), and a signal at position (12.21) ppm because of the presence of proton (SH), then the solvent signal DMSO- d_6 at 2.49 ppm, as shown in Figure 13.



MOHAMMED -MH10

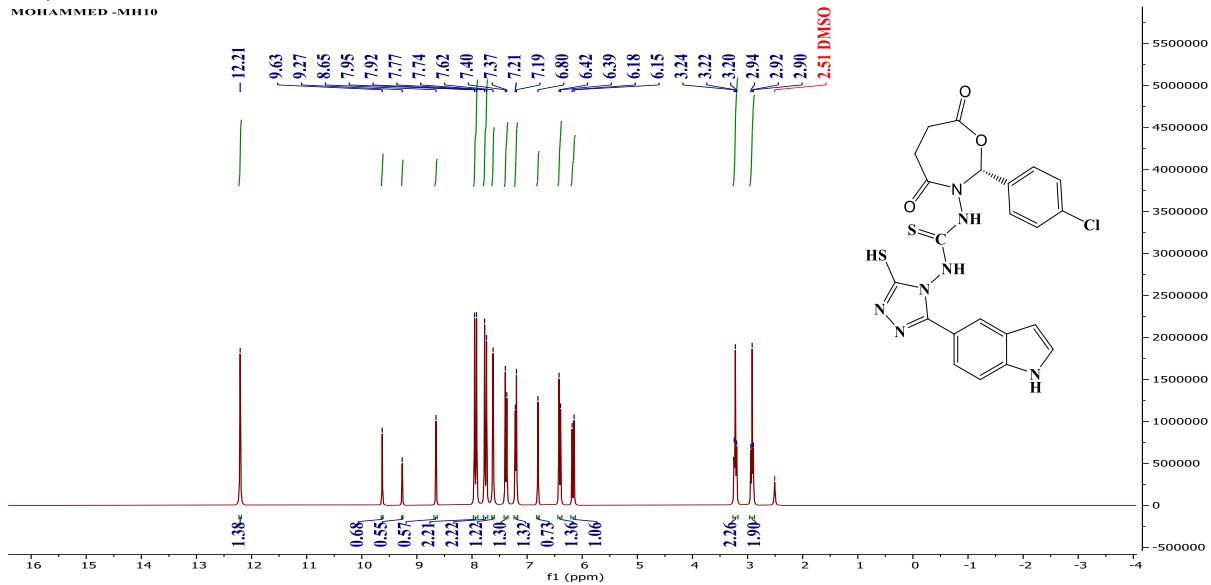


Figure (13): ¹H-NMR spectra of the substance (MH10).

In the ¹³C-NMR spectrum of MH10, two signals were observed attributed to the carbon of the (CH₂-CH₂) ring formed at positions (28.32, 34.48) ppm, a signal at (179.75) ppm because of the presence of carbonyl of the ester, a signal at 177.04 ppm attributed to the carbonyl of the amide, a signal at position (90.30) ppm because of the presence of (CH) the seven-membered ring, and the carbons of the aromatic ring appear in the range (120.11-142.63) ppm, and between the spectrum there are two signals at (119.74-115.91) ppm because of the presence of carbon of the (CH=CH) five-membered ring, and two signals at (164.08-159.95) ppm attributed to (C=N) the triazole ring. The protons of the solvent DMSO-d₆ appear between 39.37 and 40.62 ppm, as in Figure 14.

MOHAMMED -MH10

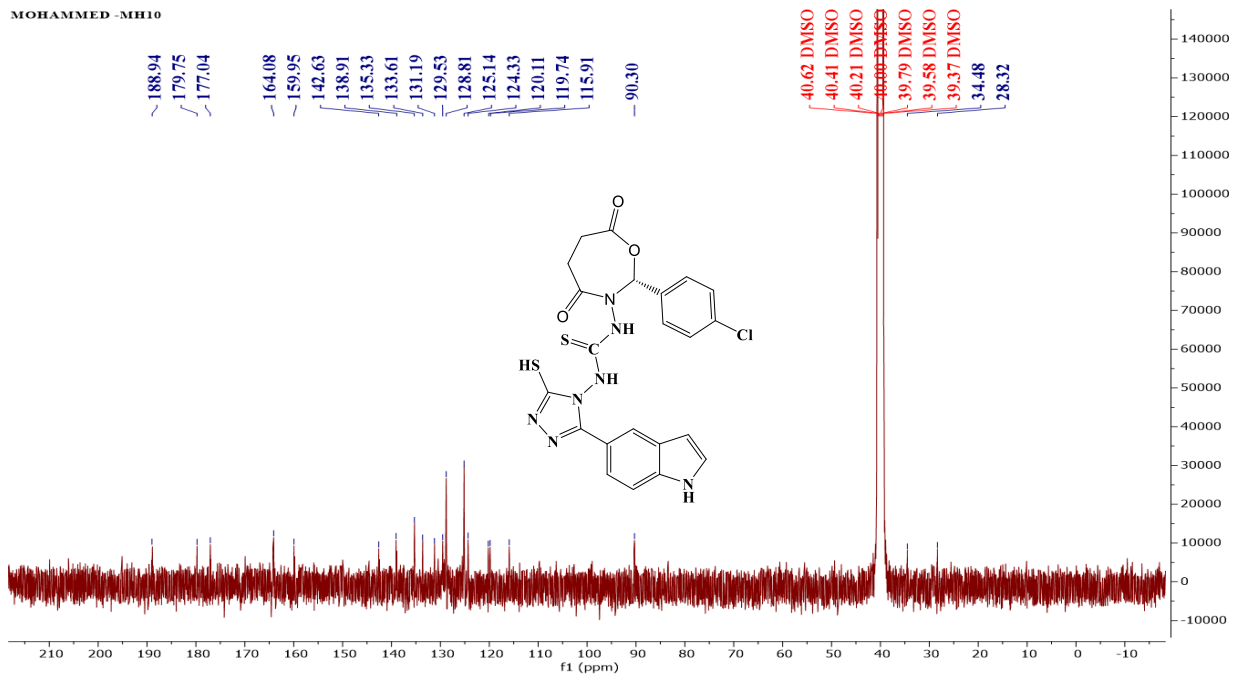


Figure (14): ¹³C-NMR Spectra of the substance (MH10).



3.3. Evaluation of the Biological Activity of Prepared Compounds

The antibacterial activity of the prepared compounds was tested using the agar diffusion method. After inoculating the culture medium with the bacterial isolates[29,30], holes were made in the Petri dishes using the cylinder measuring method (according to USP 35). Using a drill: Place the prepared compounds (40 µl) at three concentrations in each well and incubate the dish at (37°C) (24 hours) before taking the results. The readings were taken after (24) hours and (48) hours to indicate the derivatives' sensitivity. This depends on the apparent inhibitory diameter in the Petri dish surrounding the wells used; the increase in inhibitory diameter means an increase in the inhibitory diameter [31-33]. The bioavailability of the synthesised compounds was measured and compared with the inhibitory diameter of the standard antibiotics, some of which were used as control samples in the form of a solution[34-40].

Table (5): Biological efficiency of some synthesised compounds and control parameters (cm).

Comp. No.	Klebseilla pneumoniae			Staph. Epidermidis		
	0.001	0.01	0.1	0.001	0.01	0.1
MH1	0.2	0.2	1	0.1	0.2	1.1
MH2	0.2	0.5	0.8	0.2	0.2	0.8
MH3	0.3	0.8	1.2	1	1	1.5
NH5	0.2	0.5	2	0.5	1	1.5
MH8	0.5	0.5	0.8	0.5	1.2	2
MH9	0.2	0.5	1.2	1.5	1.9	2.2
MH11	0.2	0.8	1	0.5	3.5	4.5
MH12	0.4	0.8	2.3	0.8	1.6	2.2
Amoxicillin	21	22	25	25	29	33

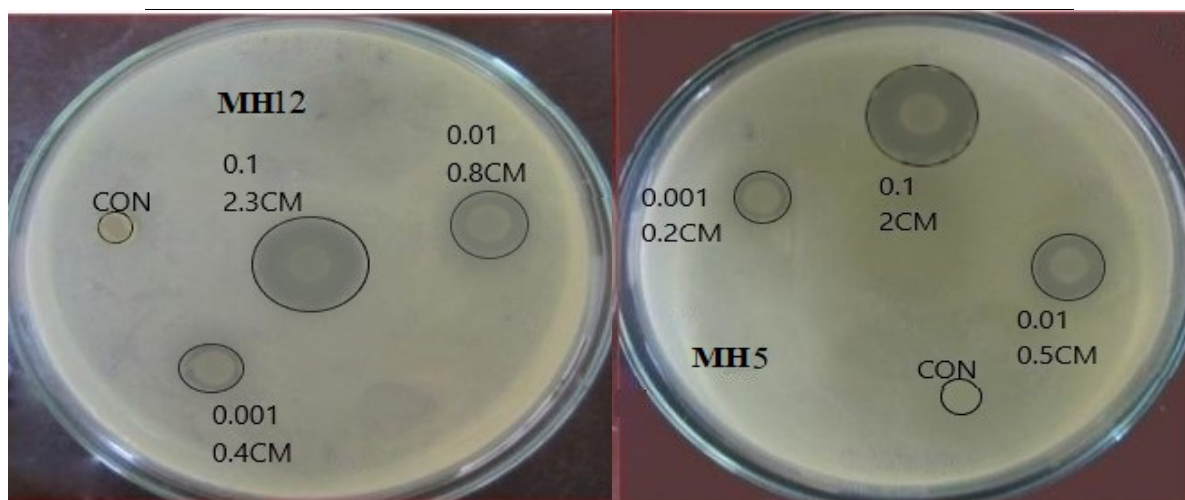


Figure (7): Biological effectiveness of the compound MH5, MH12 against bacterial K.pneumoniae.

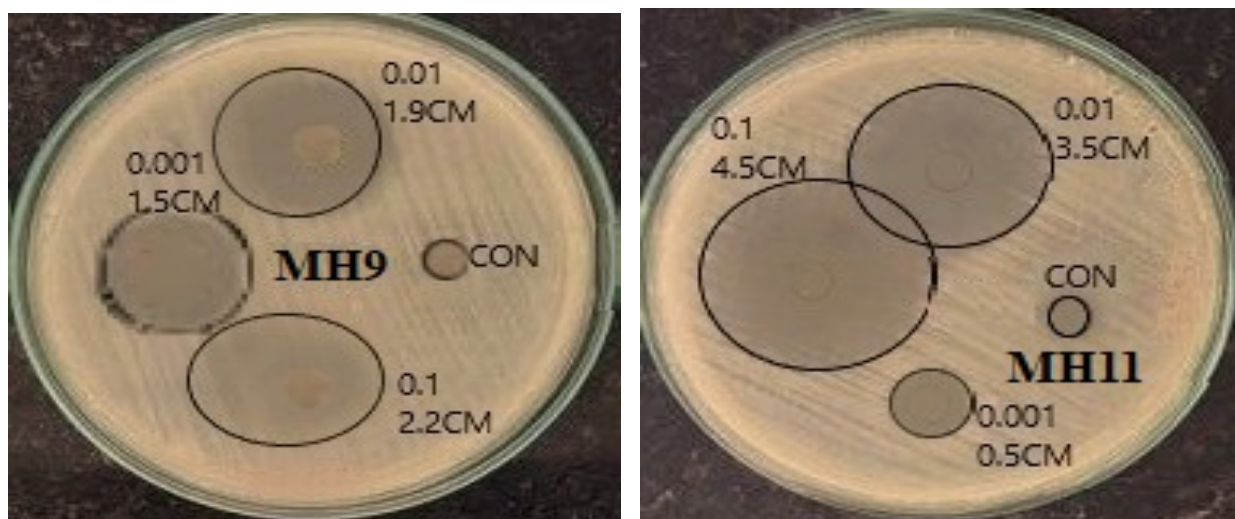


Figure (8): Biological effectiveness of the compound MH9, MH11 against bacterial *Staph. epidermidis*.

1. Conclusions

The current study applies infrared and nuclear magnetic resonance spectra to explore the bacterial efficacy of some oxazepane derivatives derived from hydrazones.

The validity of the compositions of the synthesised compounds was confirmed by the physical qualities of the melting points and colours and by spectral studies, as well as the infrared spectrum and nuclear magnetic resonance spectrum of the proton and carbon. When testing its bacterial sensitivity against bacterial species, they gave good efficacy against Gram-negative and positive bacteria in comparison with antibiotics such as *Amoxicillin*.

For future studies, it is recommended to study the possibility of applying the same techniques to explore the derivatives from other chemicals.

Conflicts of Interest: The authors declare no conflict of interest.

References

1. Khairallah, B. A., Muhammad, F. M., Saleh, J. N., & Saleh, M. J. (2024). Preparation, Characterisation, Biological Activity Evaluation, and Liquid Crystallography Study of New Diazepine Derivatives. *World of Medicine: Journal of Biomedical Sciences*, 1(7), 65-76.
2. Talluh, A. W. A. S., Saleh, M. J., & Saleh, J. N. (2024). Preparation, Characterisation and Study of the Molecular Docking of Some Derivatives of the Tetrazole Ring and Evaluation of their Biological Activity. *World of Medicine: Journal of Biomedical Sciences*, 1(7), 15-23.
3. Sathish Kumar, S., & P Kavitha, H. (2013). Synthesis and biological applications of triazole derivatives—a review. *Mini-Reviews in Organic Chemistry*, 10(1), 40-65.
4. Kumar, S., Khokra, S. L., & Yadav, A. (2021). Triazole analogues as potential pharmacological agents: A brief review. *Future Journal of Pharmaceutical Sciences*, 7(1), 106.
5. Abdul Wahed, A. S. T. (2024). Preparation and Evaluation of Bacterial Activity and Study of the Crystalline Properties of Some 1, 3-Oxazepine-4, 7-Dione Derivatives. *Central Asian Journal of Theoretical and Applied Sciences*, 5(2), 15-26.



6. Shaima H. Abdullah et al. (2024). Synthesis, Characterisation and Antibacterial Evaluation of Novel Thiazolidine Derivatives, *Journal of Angiotherapy*, 8(3), 1-9, 9501
7. Najim, D. M., Al-badrany, K. A., & Saleh, M. K. Synthesis of some new oxazepine compounds derived from cyanoethyl acetate and study their inhibitory activity against some pathogenic bacterial species. *Unpublished*.
8. Muhammad, F. M., Khairallah, B. A., & Albadrany, K. A. (2024). Synthesis, characterisation and Antibacterial Evaluation of Novel 1, 3-Oxazepine Derivatives Using A Cycloaddition Approach. *Journal of Angiotherapy*, 8(3), 1-5.
9. Al-Jubori, H. M. S. (2024). Preparation and Characterisation of Some 1, 3-Oxazepane-7, 4-Dione Derivatives and Evaluation of their Biological Activity. *EUROPEAN JOURNAL OF MODERN MEDICINE AND PRACTICE*, 4(4), 333-343.
10. Kwiecien, H., Smist, M., & Wrzesniewska, A. (2012). Synthesis of aryl-fused 1, 4-oxazepines and their oxo derivatives: A Review. *Current Organic Synthesis*, 9(6), 828-850.
11. Sager, A. G., Abaies, J. K., & Katoof, Z. R. (2023). Molecular Docking, Synthesis and Evaluation for Antioxidant and Antibacterial Activity of New Oxazepane and Benzoxazepine Derivatives. *Baghdad Science Journal*.
12. Dorababu, A. (2023). Update of Recently (2016–2020) Designed Azepine Analogs and Related Heterocyclic Compounds with Potent Pharmacological Activities. *Polycyclic Aromatic Compounds*, 43(3), 2250-2268.
13. Hassan, S. A., Aziz, D. M., Abdullah, M. N., Bhat, A. R., Dongre, R. S., Ahmed, S., ... & Jamalis, J. (2023). Design and synthesis of oxazepine derivatives from sulfonamide Schiff bases as antimicrobial and antioxidant agents with low cytotoxicity and hemolytic prospective. *Journal of Molecular Structure*, 1292, 136121.
14. Demaray, J. A., Thuener, J. E., Dawson, M. N., & Sucheck, S. J. (2008). Synthesis of triazole-oxazolidinones via a one-pot reaction and evaluation of their antimicrobial activity. *Bioorganic & medicinal chemistry letters*, 18(17), 4868-4871.
15. Khurshid, M. N., Jumaa, F. H., & Jassim, S. S. (2022). Synthesis, characterisation, and evaluation of the biological activity of tetrazole compounds derived from the nitrogenous base uracil. *Materials Today: Proceedings*, 49, 3630-3639.
16. Talluh, A. W. A. S., Saleh, J. N., & Saleh, M. J. (2024). Preparation, Characterisation and Evaluation of Biological Activity and Study of Molecular Docking of Some New Thiazolidine Derivatives.
17. Jumaa, F. H., & Shawkat, S. M. (2022, November). Synthesis, assess biological activity and laser efficacy of some new bis-1, 3-oxazepene 4, 7-dione derivatives. In *AIP Conference Proceedings* (Vol. 2394, No. 1). AIP Publishing.
18. Dalaf, A. H., Saleh, M. J., & Saleh, J. N. (2024). Green Synthesis, Characterization, And Multifaceted Evaluation Of Thiazolidinone Derivatives: A Study On Biological And Laser Efficacy. *European Journal of Modern Medicine and Practice*, 4(7), 155-168.
19. Saleh, M. J., Saleh, J. N., & Al-Badrany, K. (2024). Preparation, characterisation, and evaluation of the biological activity of pyrazoline derivatives prepared using a solid base catalyst. *European journal of modern medicine and practice*, 4(7), 25-32.
20. Saleh, J. N., & Khalid, A. (2023). Synthesis, characterisation and biological activity evaluation of some new pyrimidine derivatives by solid base catalyst AL₂O₃-OBa. *Central Asian Journal of Medical and Natural Science*, 4(4), 231-239.
21. Talluh, A. W. A. S., Saleh, M. J., Saleh, J. N., Al-Badrany, K., & mohammed saleh Al-Jubori, H. (2024). Preparation, characterisation, and evaluation of the biological activity of new 2, 3-dihydroquinazoline-4-one derivatives. *EUROPEAN JOURNAL OF MODERN MEDICINE AND PRACTICE*, 4(4), 326-332.



22. Talluh, A. W. A. S. (2024). Preparation, Characterisation, Evaluation of Biological Activity, and Study of Molecular Docking of Azetidone Derivatives. *Central Asian Journal of Medical and Natural Science*, 5(1), 608-616.
23. Saleh, M. J., & Al-Badrany, K. A. (2023). Preparation, characterisation of new 2-oxo pyran derivatives by AL₂O₃-OK solid base catalyst and biological activity evaluation. *Central Asian Journal of Medical and Natural Science*, 4(4), 222-230.
24. Muhammad, F. M., Khairallah, B. A., Saleh, M. J., & Saleh, J. N. (2024). Preparation and Characterisation of New Rings of Oxazine Derivatives and Studying Their Biological and Laser Effectiveness and Molecular Docking. *Central Asian Journal of Theoretical and Applied Science*, 5(4), 190-201.
25. Sathish Kumar, S., & P Kavitha, H. (2013). Synthesis and biological applications of triazole derivatives—a review. *Mini-Reviews in Organic Chemistry*, 10(1), 40-65.
26. Shah, M. A., Uddin, A., Shah, M. R., Ali, I., Ullah, R., Hannan, P. A., & Hussain, H. (2022). Synthesis and characterisation of novel hydrazone derivatives of isonicotinic hydrazide and their evaluation for antibacterial and cytotoxic potential. *Molecules*, 27(19), 6770.
27. de Oliveira Carneiro Brum, J., França, T. C., LaPlante, S. R., & Villar, J. D. F. (2020). Synthesis and biological activity of hydrazones and derivatives: A review. *Mini reviews in medicinal chemistry*, 20(5), 342-368.
28. Vessally, E., Hosseinian, A., Edjlali, L., Bekhradnia, A., & Esrafil, M. D. (2016). New route to 1, 4-oxazepane and 1, 4-diazepane derivatives: synthesis from N-propargylamines. *RSC advances*, 6(102), 99781-99793.
29. Sattar Talluh, A. W. A., Saleh, J. N., Saleh, M. J., & Saleh Al-Jubori, H. M. (2024). Preparation and Characterisation of New Imidazole Derivatives Derived From Hydrazones and Study of their Biological and Laser Efficacy. *Central Asian Journal of Theoretical and Applied Science*, 5(4), 202-211.
30. Saleh, M. M., Saleh, J. N., Rokan, F. F., & Saleh, M. J. (2024). Synthesis, Characterization and evaluation of bacterial efficacy and study of molecular substrates of cobalt (II) complex [Co (2-(benzo [d] thiazol-2-yloxy) acetohydrazide)(H₂O)(Cl₂)]. *Central Asian Journal of Medical and Natural Science*, 5(4).
31. Talluh, A. W. A. S., Saleh, M. J., Saleh, J. N., & Al-Jubori, H. M. S. (2024). Synthesis and Characterisation of Some New Imine Graphene Derivatives and Evaluation of Their Biological Activity. *Central Asian Journal of Medical and Natural Science*, 5(4), 272-290.
32. Al-Joboury, W. M., Al-Badrany, K. A., & Asli, N. J. (2022, November). N-alkylation of substituted 2-amino benzothiazoles by 1, 4-bis (bromo methyl) benzene on mixed oxides at room temperature and study their biological activity. In *AIP Conference Proceedings* (Vol. 2394, No. 1). AIP Publishing.
33. Al-Joboury, W. M., Al-Badrany, K. A., & Asli, N. J. (2021). Synthesis of new azo dye compounds derived from 2-aminobenzothiazole and study their biological activity. *Materials Today: Proceedings*, 47, 5977-5982.
34. Saleh, R. H., Rashid, W. M., Dalaf, A. H., Al-Badrany, K. A., & Mohammed, O. A. (2020). Synthesis of some new thiazolidinone compounds derived from schiff bases compounds and evaluation of their laser and biological efficacy. *Ann Trop & Public Health*, 23(7), 1012-1031.
35. Abdullah, S. H., Salih, M. M., & Khalid, A. Synthesis, Characterization and Antibacterial Evaluation of Novel Thiazolidine Derivatives.
36. Al-Tufah, M. M., Jasim, S. S., & Al-Badrany, K. A. (2020). Synthesis and Antibacterial Evaluation of some New Pyrazole Derivatives. *Prof.(Dr) RK Sharma*, 20(3), 178.



37. Al Rashidy, A. A. M., Al Badrany, K. A., & Al Garagoly, G. M. (2020, August). Spectrophotometric determination of sulphamethoxazole drug by new pyrazoline derived from 2, 4-dinitro phenyl hydrazine. In *Materials Science Forum* (Vol. 1002, pp. 350-359). Trans Tech Publications Ltd.
38. Al-Joboury, N. A., Al-Badrany, K. A., Hamed, A. S., & Aljoboury, W. M. (2019). Synthesis Of Some New Thiazepine Compounds Derived From Chalcones And Evaluation There Biochemical And Biological Activity. *Biochemical & Cellular Archives*, 19(2).
39. Al-Badrany, K. A., Mohammed, A. S., & Alasadi, Y. K. (2019). Synthesis of some new 1, 3, 4-oxadiazole compounds derived from 1H-imidazole and study their biological activity. *Eurasian Journal of Biosciences*, 13(1), 501-507.
40. Al Rashidy, A. A. M., Al Badrany, K. A., & Al Garagoly, G. M. (2020, August). Spectrophotometric determination of sulphamethoxazole drug by new pyrazoline derived from 2, 4-dinitro phenyl hydrazine. In *Materials Science Forum* (Vol. 1002, pp. 350-359). Trans Tech Publications Ltd.
41. Al-Badrany, K. A. (2024). The use of 2-aminopyrazine as a basic nucleophile for the preparation of new derivatives of the 5, 6-dihydropyridine-2 (1h)-ylidene) cyanamide ring, their diagnosis, and evaluation of their bacterial efficacy. *European journal of modern medicine and practice*, 4(5), 508-518.